IEEE Access
Multidisciplinary | Rapid Review | Open Access Journal

Received 22 December 2023, accepted 9 January 2024, date of publication 15 January 2024, date of current version 22 January 2024.

Digital Object Identifier 10.1109/ACCESS.2024.3353046

RESEARCH ARTICLE

Cooperative Unmanned Aerial and Surface Vehicles for Extended Coverage in Maritime Environments

MATHEUS C. SANTOS[1,2], (Member, IEEE), BEN BARTLETT[1,2], (Member, IEEE), VINCENT E. SCHNEIDER[3], FIACHRA Ó. BRÁDAIGH[4], BENJAMIN BLANCK[5], PHILLIPE C. SANTOS[2,6], PETAR TRSLIC[1,2], JAMES RIORDAN[7], AND GERARD DOOLY[1,2], (Member, IEEE)

[1]School of Engineering, University of Limerick, Limerick, V94 T9PX Ireland
[2]Centre for Robotics and Intelligent Systems (CRIS), University of Limerick, Limerick, V94 T9PX Ireland
[3]Sea Traffic and Nautical Solutions, Fraunhofer Center for Maritime Logistics and Services (CML), 21079 Hamburg, Germany
[4]XOCEAN, Rathcor, Louth, A91 DVT0 Ireland
[5]SEC 11—Research and Development Hamburg Port Authority, 20457 Hamburg, Germany
[6]Department of Electrical Engineering, Federal Institute of Sergipe, Estância 49200-000, Brazil
[7]ALMADA Research Centre, School of Computing, Engineering and Physical Science, University of the West of Scotland, G72 0LH Glasgow, U.K.

Corresponding author: Matheus C. Santos (matheus.santos@ul.ie)

This work was supported in part by the European Commission's Horizon 2020 Project RAPID under Grant 861211, and in part by the Enterprise Ireland's Disruptive Technologies Innovation Fund (DTIF) Project GUARD under Grant DT2020 0286B.

ABSTRACT Maritime operations, such as ship hull inspections, infrastructure assessments, and rapid response to emergencies, often expose humans to hazardous environments. The deployment of unmanned vehicles offers a potential solution to mitigate risks and reduce operational costs in such scenarios. Collaborative efforts between Unmanned Aerial Vehicles (UAVs) and Unmanned Surface Vehicles (USVs) can enhance mission endurance and portability. This paper introduces a cooperative UAV-USV system designed to expand the operational coverage area. It leverages off-the-shelf satellite-based technology to establish robust communication links between UAVs, USVs, and the ground station. This connection facilitates the development of an autonomous launch and recovery system, relying on GPS and visual servoing. Furthermore, the system incorporates a Battery Hot Swap-system (BHS) on the USV, allowing the UAV to resume its mission within 3 minutes. The effectiveness of this proposed solution was demonstrated through successful inspection trials conducted at the port of Hamburg, Germany.

INDEX TERMS Unmanned aerial vehicles, unmanned surface vehicles, cooperative systems, UAV, USV, autonomous landing, autonomous navigation.

I. INTRODUCTION

Over the last few years, there has been a rapid development of Unmanned Aerial Vehicles (UAV). Interest in these systems comes from the variety of applications for UAVs that are used for military and civilian purposes, such as surveillance, environment monitoring, search, exploration, inspection, cargo delivery, etc [1], [2].

The maritime industry is one of the main use cases for UAS technology since unmanned systems can safely inspect and explore dangerous or inaccessible areas for humans such as ship hulls, water ballast tanks, port infrastructure, and bridge pillars [3]. The use of drones for inspections allows for the reduction of risk, time, and cost of operation [4].

Commercial drones typically used in the maritime environment have the drawback of a short flight time, which can affect their ability to cover large areas [3], [5]. On average, a single flight can reach up to a distance of 10 km, which should be sufficient for covering Europe's two largest ports, Rotterdam and Hamburg [5]. However, during inspection operations, the mapping path may need an overlap, which reduces significantly the coverage area. For instance, when

The associate editor coordinating the review of this manuscript and approving it for publication was Eyuphan Bulut.

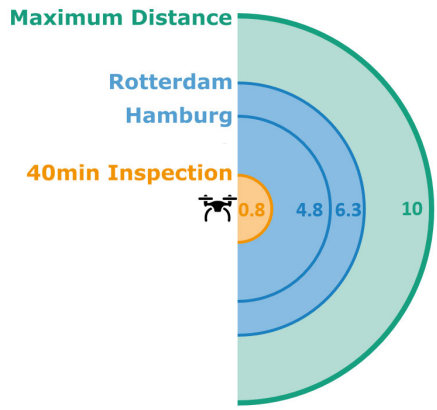

FIGURE 1. Coverage areas in kilometers. Drone range for regular flights and inspections in green and yellow, respectively. Europe ports in blue.

operating at a height of 120 meters with a 60% overlap, a 40-minute inspection can cover up to 2 km^2, highlighting the need for multiple flights to achieve full coverage, as shown in Figure 1.

During maritime operations, every target is surrounded by water, enabling Unmanned Surface Vehicles (USVs) to serve as a viable solution for significantly extending the inspection range, carrying heavy payloads, and achieving long mission endurance [6]. A cooperative UAV-USV system, where the USV serves as a platform for take-off and landing, can combine the advantages of both solutions [6], [7], [8].

It is well known that the landing phase is the most dangerous task for manned and unmanned flights. The task accuracy must be high to avoid the risk of a crash. Besides, the landing has a limited amount of time and space to be done. Thus, autonomous landing has been addressed by several research groups in the last couple of decades [9].

Precision and safety requirements in the landing phase on a USV do not allow the system to be based only on GPS data. Computer vision has been highlighted in the development of unmanned aerial vehicles as an important component of the control system, due to the rich information provided by visual information for autonomous landing and obstacle avoidance [10], [11].

Recent research has focused on the development of landing systems with landing pads fixed with markers, such as the Aruco markers [12]. These markers are designed to provide the system with information about the aircraft's position and orientation [13]. However, the visual estimation implies in the system the need to have the marker in the field of view (FOV) during the entire landing phase.

Current automated inspection solutions in the literature face challenges in achieving a fully autonomous workflow, often relying on a pre-existing 3D digital representation of the environment and encountering limitations in operational time [14], [15]. Key aspects crucial for sustained operations, such as recovery, recharging, and relaunching, are frequently overlooked in experimental phases.

Some commercial solutions address these challenges: the DJI Dock [16] aims to enhance flight time by enabling a 10-90% drone charge in just 25 minutes. Energy Robotics [17] offers a "drone-in-a-box" solution with a 90-minute recharge time, utilizing a DJI MAVIC 2 Enterprise and leveraging an existing 3D environmental model for autonomous inspections. Perceptual Robotics [18] specializes in wind turbine inspection, dynamically planning paths based on previous knowledge of the turbine model and visual feedback without a dedicated recharging solution.

To unlock the full potential of UAVs for maritime operations, it is crucial that the developed systems aim for a high degree of automation, requiring minimal input or supervision from the operator. This emphasis on a reliable automated system becomes preeminent, especially given the often challenging and inaccessible nature of operational areas in maritime environments. Therefore, prioritizing research and system development efforts toward achieving both automation and high endurance is essential for effective and efficient maritime inspection.

This paper presents the solution developed under the Risk-aware Automated Port Inspections Drones (RAPID) project to extend the range of operations described in previous work [19], [20]. Our research focuses on the development of a fully automated UAV-USV Cooperative system for the autonomous inspection of maritime infrastructure. This system enables the drone to conduct inspections and safely return to the USV, performing autonomous landings from altitudes of up to 100 meters. To enhance operational endurance, the USV is equipped with a Battery Hot Swap-system (BHS), facilitating the quick replacement of fully charged batteries within a mere 3 minutes, thus ensuring uninterrupted operation [5]. The system's performance is validated through real-world trials designed to meet the rigorous requirements of the Hamburg Port Authority.

The principal contributions of this study can be summarized as follows:

- Cooperative UAV-USV System. Establishing a stable connection between vehicles on the same network allows for real-time exchange of telemetry information.
- GPS and Vision-based Autonomous Landing. The USV GPS position allows the landing phase to start within 10 m on the latitude-longitude plane. In terms of altitude, the system showcases visual detection capabilities at heights of up to 100 meters from the target. At full capacity and adhering to current regulations, the system can initiate the landing phase from the maximum allowable altitude.
- Extended range of operation workflow. The Battery Hot Swap-system in addition to the cooperative take-off and landing capabilities allows the inspection to be performed based on the endurance of the surface vehicle.

The paper is structured as follows: Section II presents the state-of-the-art of UAV-USV cooperative systems and autonomous landing; Section III describes the proposed solution in this paper; Section IV is dedicated to presenting all the setup used within the scope of this paper and the

autonomous landing process; The results and discussions of the experiments performed in this paper are shown in Section V; Finally, conclusions and propositions for the future are presented in Section VI, followed by the bibliographic references.

II. RELATED WORK

This section is dedicated to presenting a review of the cooperative UAV-USV systems and autonomous landing, showing the state-of-the-art and the main approaches developed to solve these problems.

A. COOPERATIVE UAV-USV SYSTEMS

Unmanned vehicles (UVs) have garnered attention from industry and researchers across different scenarios, including Aerial, Ground, Surface, and Underwater environments, owing to their capacity for risk reduction, cost-effectiveness, and extended reach [21], [22]. Each class of UV presents its unique challenges and advantages. A cooperative approach may enhance resource utilization and further augment their capabilities [6].

This paper focuses on the cooperation between UAVs and USVs in maritime environments, an emerging solution that has recently gained attention. In reference [8], an effective communication framework is proposed for maintaining formation. This framework utilizes a distributed dynamic network topology designed so that the ground control is connected to a USV and UAV gateway, each containing all the information of its respective vehicles. All the experiments are carried out in a simulated environment.

In the context of a search and rescue task, researchers in [23] propose an intragroup communication architecture that utilizes both UAVs and USVs to relay connections within the group. Additionally, a path planner is introduced to coordinate multiple vehicles and facilitate comprehensive coverage of the desired area within a simulated environment.

Monitoring and managing algae in rivers, lakes, and other freshwater environments is becoming a growing challenge. In [24], researchers conducted a comparative study involving concurrent surveys using both UAVs and USVs. Furthermore, in [25], the UAV takes the lead by initiating the mission and conducting visual algae detection. Once the target is located, the USV is deployed to the algae's location for removal.

During maritime operations, it is worth mentioning the use of Unmanned Underwater Vehicles (UUVs), also known as Autonomous Underwater Vehicles (AUVs), as important assets for a comprehensive evaluation of maritime structures. Particularly in the assessment of structures partially submerged in water, such as ship hulls, bridges, ports, and offshore wind turbines [26], [27], [28], [29].

A collaborative approach involving UAVs, UUVs, and ROVs was implemented for maritime spill response, as detailed in [7]. This deployment served as a case study during the Cathach exercise—a multi-agency marine incident response training program conducted on the Shannon Estuary in Ireland. The exercise featured the utilization of advanced robotic platforms in collaboration with state agencies to simulate a marine incident scenario. To facilitate real-time communication, an ad-hoc high-bandwidth radio communications infrastructure was established to relay information promptly from the incident location to a ground station. The ground station played a pivotal role in decision-making processes, which were subsequently transmitted to the UVs on-site.

In reference [30], a cooperative system for water pollution monitoring is introduced to extend the UAV's cruise range. This system incorporates a wireless charging mechanism integrated with the USV. Notably, while this setup extends the UAV's flight time, it is important to note that the charging time was not addressed in the study. This aspect is critical to consider since prolonged charging times can render the system inoperative for extended periods, potentially resulting in operational delays of tens of minutes. To mitigate this challenge, a battery-swapping approach followed by subsequent charging could dramatically reduce downtime and improve system responsiveness.

Furthermore, it's important to note that the paper does not explore into the details of the approach used for launching and recovering the UAV from the USV. The capability for efficient and safe launch and recovery of the UAV is a crucial aspect of any cooperative system.

B. LAUNCH AND RECOVERY

Identifying a suitable location for launching and recovering the UAV in a maritime environment can be a complex task. Therefore, employing the USV as a secure platform emerges as a practical solution to ensure the safety and endurance of operations.

The work developed in [31] presents a platform design for coupled USV-UAV systems. The system incorporates four ultrasound sensors positioned on the USV, primarily serving the purpose of detecting and guiding the UAV during the landing phase. It's important to mention that the paper does not explore aspects such as GPS positioning and the approaching phase. Despite the successful tests, the landing phase does have an average duration of approximately 3 minutes. Additionally, the applicability of this approach is somewhat limited, as it is most effective when the UAV is already in close proximity to the USV.

The design of a cooperative platform named Transformer is proposed in [32]. This platform establishes communication between the UVs through a radio frequency (RF) module. Based on the shared information, the UAV can return to the USV and initiate the landing procedure, which will be assisted by a pilot onshore. Additionally, a wireless charging platform is integrated into the USV, enabling extended flight times. This platform is still in the early stages, and the paper primarily presents results from simulation tests.

Due to the inherent uncertainty of GPS positioning in the maritime environment, a hybrid Visual-GPS approach proves to be the most suitable solution. In [33], a swarm of VTOL

fixed-wing UAVs employs this approach for precise landings on a USV, facilitated by RF communication. A similar methodology is presented in [34], with a single UAV and the use of an infrared beacon as the target on the USV. It's worth mentioning that both of these projects are in their early development stages, with experiments primarily conducted in beachfront settings.

To the best of our knowledge, the cooperative approach presented in [35] represents the most comprehensive solution for a launch and recovery system. During the approaching phase, the system utilizes GPS information from the USV, transitioning to visual navigation upon recognizing a marker. Successful tests of this approach were carried out on a lake, employing a HUSTER-30 ASV and a DJI M-100 UAV with an average starting landing height of approximately 6 meters. It's important to mention that the paper does not offer a solution for extending the UAV's time of flight.

Based on the current literature the main components of a Cooperative UAV-USV system with launch and recovery capability are reliable communication and landing pad identification. The simplest way to build a landing pad for visual servoing is to attach a single marker as the target.

As shown in [1] a landing system was built for a static target with a single Aruco marker and performs simulation and on-site testing. In [36] is proposed a system for a moving target with a single Aruco marker through simulation. The disadvantage of a system with a single Aruco marker is that a small marker makes it difficult to detect at large distances and a big marker makes it difficult to detect at close range.

In order to avoid the problem of losing the marker, other researchers compose systems with more than one marker. In [37], two Aruco markers are attached to the landing pad. A big one for long-range detection and a small one for close range. The system can detect the landing pad up to 20 m and keep at least one marker during the entire landing phase. The system developed by [9] uses several Aruco markers with different sizes coupled to a mobile robot for landing tested indoors.

A ship heave motion simulator was developed in [38] to evaluate the performance of a landing system in a shipboard environment. The landing pad proposed has two different Aruco markers with the small one placed on the center of the big one. The tests presented in this paper are performed indoors.

Other patterns of markers may be used for visual servoing. In [39] a dynamic landing pad device is presented which communicates with the UAV and uses a simple marker (Whycon [40]) for long-range and swaps to the Aruco marker at close range. The dynamic component also allows for a change in the size of the marker according to the distance to the aircraft.

An ellipsoidal marker with an "x" at the center is used on [41]. In this paper, a monocular camera and Time of Flight (ToF) sensors are used for an autonomous landing on a moving platform. Assuming the route, speed, and directions of the ground vehicle are known, the ToFs are used to perceive the vehicle below the drone which activates the landing procedure. Notably, the paper does not specify the maximum altitude achieved by the system. However, during the experiments, the initial vertical distance to the target is set at 3.5 meters.

FIGURE 2. DJI matrice 300 (UAV) - used during RAPID project.

A color-based landing pattern is presented in [42], tested for altitudes between 20 cm and 150 cm indoors. In [43] a new pattern more suitable for low light conditions is tested successfully in different light conditions (day and night) and a maximum height of 10 m. A pattern composed of four LEDs in a T-shape is presented in [44]. This pattern can be detected using an infrared camera, allowing its detection from 15 cm to 250 cm, and may be useful in foggy environments.

In summary, there is a gap in the literature for a fully automated UAV system capable of performing continuous operations within the challenging maritime environment with trials that emulate the demands of real-world scenarios.

III. EXTENDED OPERATION RANGE

This section introduces the cooperative UAV-USV system proposed as part of the RAPID project, designed to extend operational range. RAPID targets various use cases such as ship hull and infrastructure inspection, emission monitoring, and fast response to emergencies. These applications require a suite of sensors, including LiDAR, cameras, infrared cameras, and gas probes [45]. To meet these requirements, we have selected the DJI Matrice 300 (M300) drone, a popular choice in the market due to its specifications. The M300 (shown in Figure 2) has an average flight time of 45 minutes and the capacity to carry up to three payloads simultaneously.

The RAPID project has demonstrated its proficiency in infrastructure inspection within the maritime environment using UAV technology. In [46], a bridge survey was conducted using a LiDAR sensor along the coast of Wicklow, Ireland. Additionally, in [19], the project introduced an innovative approach to photogrammetric surveys of previously unknown infrastructures. This two-stage survey begins with the creation of a low-definition 3D model using standard photogrammetric procedures from a significant height. Subsequently, a path-planning algorithm is employed to execute a close-quarter inspection, resulting in the generation of a high-definition 3D model.

FIGURE 3. XOCEAN vehicle (USV) with a battery hot Swap-system and landing pad - used during hamburg trials.

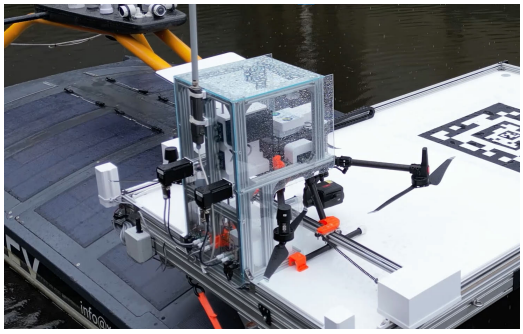

FIGURE 4. UAV locked and secured onto the hot-swap system coupled to the USV.

Finally, a real-time crack detector is presented in [20] for monitoring critical port infrastructure, with a demonstration conducted at a lock in the Port of Hamburg, Germany. Throughout the RAPID project, all developments were deployed using two primary platforms: the Mobile SDK, which utilizes the remote controller as the processing unit, or an NVIDIA Jetson NX integrated onto the drone.

The main limitations of the UAV system revolve around its relatively short flight time and the distance between the target and the launch point. To address these challenges, we have developed a cooperative solution involving a USV. The XOCEAN USV, shown in Figure 3, is a commercially available USV with an impressive track record, with more than 100.000 operational hours and covering 600.000 kilometers overseas. This robust vehicle is capable of handling heavy payloads and ensuring safe offshore operations for extended periods, making it an ideal platform for launching and recovering UAVs [47].

The USV is equipped with a satellite-based internet connection, ensuring a reliable network connection, even in remote offshore areas. Additionally, an RF module is used through the remote controller (RC) coupled to the USV enabling it to maintain a connection with the UAV at distances of up to 11.5 km. It's worth mentioning that all decision-making processes occur directly between unmanned vehicles, and the data received at the ground station serves only for visualization purposes.

A local network is established on the USV to facilitate the exchange of telemetry data between UVs. Subsequently, all the information is transmitted to the UAV using DJI interconnected SDKs. On the onboard computer, the Robot

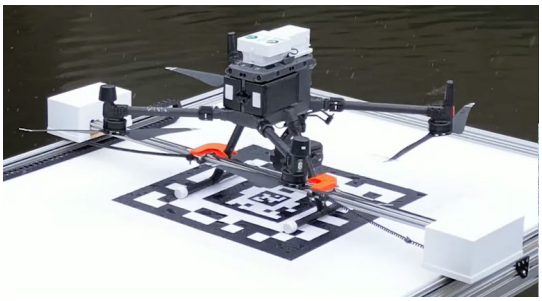

FIGURE 5. BHS actuators align and grab the UAV.

Operating System (ROS) is employed to execute autonomous tasks. Furthermore, all UVs' data are efficiently relayed to the ground station through a clientless remote desktop gateway.

Once communication is established, it's imperative to define the approach for launch and recovery. In our cooperative system, the Battery Hot Swap-system (BHS), as detailed in [5] and [48], is seamlessly integrated with the USV, providing a secure docking location for the UAVs, as can be seen in Figure 4. The BHS process involves aligning the UAV laterally and longitudinally, inserting the UAV into the BHS, sequentially swapping the UAV's batteries, and finally, redeploying the UAV to its take-off position.

The alignment process commences immediately after the landing phase. It begins with a longitudinal movement from stern to bow, aligning the UAV with the grippers. Subsequently, the grippers initiate lateral movement to locate and secure the drone, adjusting as needed to center it by aligning the landing legs with the middle axis of the landing platform, as can be seen in Figure 5. The final step involves a translational motion from the landing platform toward the BHS, ensuring the UAV is securely locked in place.

An intricate series of micro-motions ensues to unlock the battery safety lever, remove and replace the first battery, and subsequently, the second battery. The process concludes with closing the battery safety lever, achieving a hot-swap with a fully charged set of batteries without the need to power off the drone. This seamless battery replacement procedure is completed in under 3 minutes.

After the swap is finished, the UAV remains securely fastened to the platform (Figure 5) until an operational request is initiated. Additionally, the BHS also features a charging system that can recharge the used batteries directly from the USV, significantly extending the UAV's time of flight, in alignment with the endurance of the USV.

Based on the three pillars of the cooperative system - the UAV, USV, and BHS - the operational workflow, shown in Figure 6, commences with the UAV securely housed and locked onto the BHS while the USV navigates to the designated operation location. Upon reaching the desired position, the UAV is carefully maneuvered to the launch spot, from where it takes off. Following the completion of the operation, the UAV returns to the GPS coordinates of the USV, initiating the visual landing procedure. After a successful landing, the BHS platform takes over the task of recovering the UAV and executing the hot-swap.

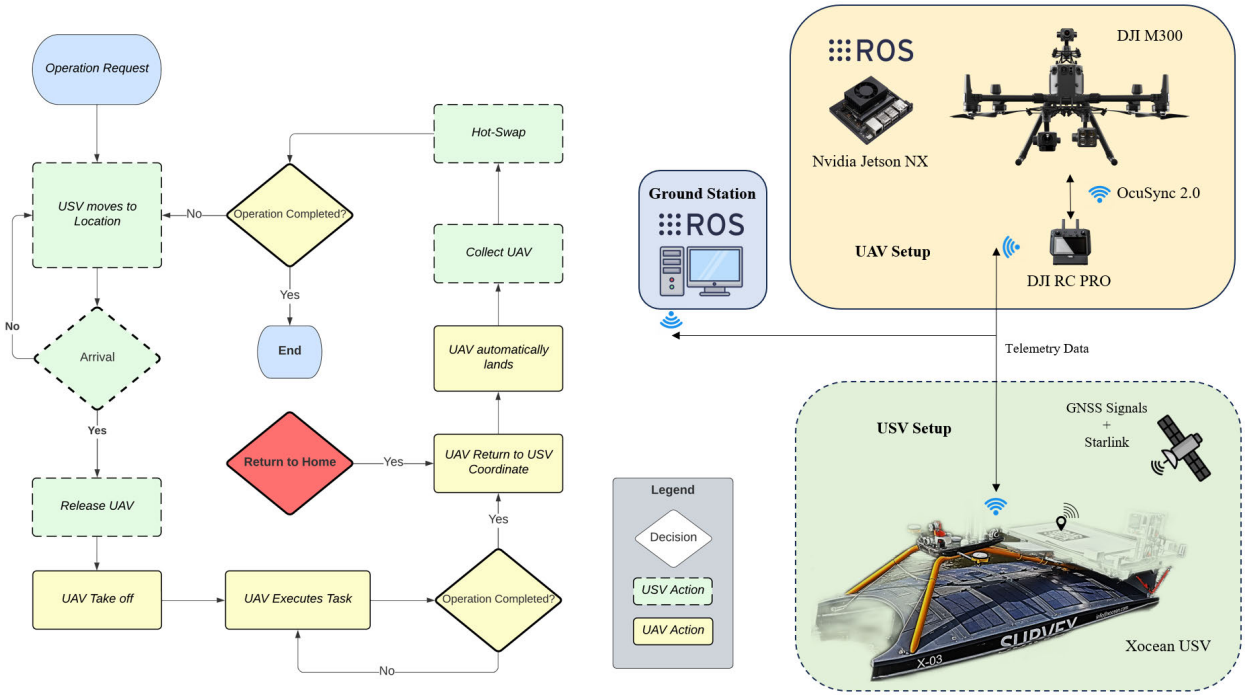

FIGURE 6. Proposed architecture and workflow for cooperative operations.

A dedicated interruption system is integrated into the overall setup to handle situations requiring a return to home. Such interruptions may occur in the event of low battery levels or a loss of connection to the RF module. When an interruption is triggered, the UAV promptly returns to the USV and initiates the landing procedure. This ambiguity in the landing trigger means that, after a hot swap, the mission can be resumed if necessary.

The proposed solution offers the potential to significantly enhance the efficiency and safety of UAV operations in maritime environments. Through cooperation with the USV, the UAV can be efficiently deployed at the targeted site and execute multiple flights, benefitting from the hot-swap system.

IV. LANDING PHASE

One of the crucial phases of the approach proposed in Section III is the landing phase. This section presents the design of the landing pad and outlines the workflow for the landing procedure.

A. LANDING PAD

The project for designing the landing pad begins with the tag selection. A recent development in this field is the introduction of a new class of tags known as Fractal Markers, proposed in [49]. These markers have been specifically designed to ensure reliable detection across significant distance variations. As shown in Figure 7, the unique design of a tag inside another tag offers the capability for both long-range and short-range detection.

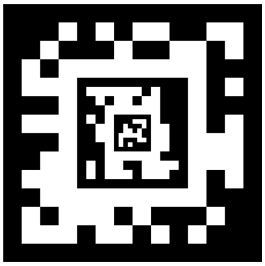

FIGURE 7. Fractal marker.

In most real-world operations, the risk of collision with vessels or marine infrastructure is a significant concern. This risk is particularly intensified during the UAV's return from the operation location to the USV's position. To mitigate this risk, the UAV is required to operate at high altitudes. Consequently, this work is focused on detecting the landing pad from substantial heights, even up to 60 meters. In line with these requirements, a fractal marker of 800 mm^2 has been chosen as the tag.

The landing platform measures 2.5 m x 1.43 m, with a dedicated area of 1.05 m x 1.43 m reserved for the swap station. This configuration provides the UAV with a landing zone of 1.45 m x 1.43 m. The marker is strategically positioned at the center of the landing zone to maximize the distance from the edges of the landing area. In terms of mechanical interface, the BHS system ensures a vertical clearance of at least 6 cm between the drone's propellers and the BHS. This design safeguards against potential inaccuracies during landing, allowing the drone's arms to extend over the platform without posing any threat to the UAV or USV.

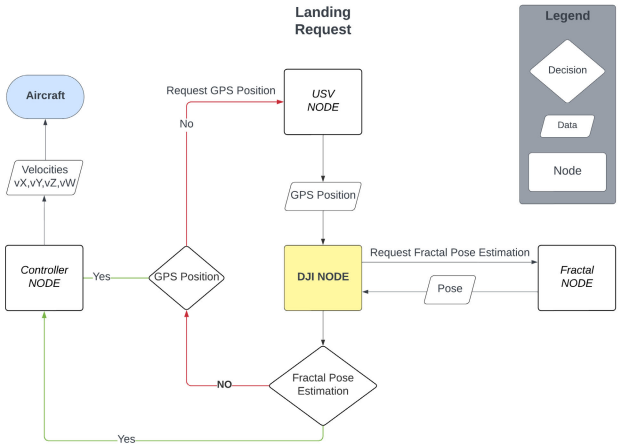

FIGURE 8. Landing phase workflow. The flow starts with the DJI node (yellow) and ends with the aircraft action (blue).

B. WORKFLOW

The system architecture is presented in Figure 6. The Jetson NX board communicates with the USV through the RC controller and requests its position. The workflow begins once the GPS coordinates become available.

The flowchart shown in Fig. 8 was developed to describe the high-level control of the aircraft during the landing phase. Each process in the flow represents a ROS node that communicates with each other according to the behaviors projected on the workflow. The DJI node (highlighted in yellow) is the main node of the system, responsible for managing all the information. This node is connected to the pose estimation and USV nodes and it is responsible for all the decision-making process.

Upon receiving a landing request, the main node initiates a request to the fractal node for pose estimation. In cases where visual detection is unsuccessful, the main node then requests the USV GPS coordinates. Subsequently, the controller node receives either the pose or the GPS position, and it calculates x, y, z, w velocities within the body frame, with (x, y, z) representing the axis of the coordinate frame and w the yaw component. It is worth mentioning that the pose estimation process has the highest priority, ensuring that visual servoing is executed when the marker is detected.

C. VISUAL SERVOING

In an autonomous flight, the landing procedure starts after the completion of a desired task. We anticipate that the aircraft will have completed this task at a distance from the designated landing area. As a result, the initial step in our landing procedure involves utilizing GPS information to guide the UAV to the USV where the landing pad can be detected by the vision sensors.

After reaching the landing area, the system proceeds to engage in visual servoing. To facilitate control actions, the transformation between coordinate frames is established. In our system, we assume that the camera is fixed, due to its gimbal, and the body coordinate frame aligns with the camera frame. Notably, the DJI SDKs offer high-level control, ensuring that the pose and velocity estimation of the aircraft align with the camera. In this paper, we make use of two reference frames: the landing pad reference frame $\{L\}$ and the body-fixed frame $\{B\}$, related by the transform $\mathbf{T}_B^L$.

The position of the landing pad serves as the origin, denoted as o in our system, and is determined through the detection of the Fractal marker. Consequently, the primary objective of the landing task is to minimize the error relative to this origin. As a result, the estimated of the UAV can be assigned as the position error,

$$\mathbf{E}_p = \mathbf{T}_B^L \times p_B, \tag{1}$$

where p_B is the UAV position in body frame.

In order to perform the control of the UAV we propose a simple proportional speed controller with a single nonlinear activation function σ, a sigmoid based on the hyperbolic tangent:

$$\sigma(x) = tanh(x). \tag{2}$$

The xy axis component from Eq. 1 is then used in velocities control equations to minimize the position error,

$$\mathbf{V}_{xy} = \alpha\sigma(E_p K), \tag{3}$$

which α changes the amplitude of the controller and the K factor determines the slope of the function at the origin, and can change the functional behavior from slowly rising transitions ($K \to \infty$) to one of a unit step function ($K \to 0$).

Due to the large height range the control for the z axis is partitioned into distinct zones. A descending cone-based region is defined, as shown in Figure 9, based on height (h) and radius tolerance (r). During each frame inference, the relative position from the drone to the descending region is quantified using

$$z_k = \begin{cases} 1, & E_p \leq r(h) \\ 0, & E_p > r(h), \end{cases} \tag{4}$$

where z is an array of events, k is the frame number and $r(h)$ is a function that returns the radius tolerance based on the actual height. Using equation (4) a time window is created as

$$t_k = \sum_{n=k-N}^{k} z_n, \tag{5}$$

where N is used to set the duration which is dependent on the frame rate. This time window is used to define a minimum time required to start the descending phase based on a threshold (D). Once the threshold is reached, a function that outputs a constant velocity $v_z(h)$ along the z-axis based on the current zone is calculated as:

$$V_z = \begin{cases} -v_z(h), & t_k \geq D \\ 0, & t_k < D \end{cases} \tag{6}$$

The last component of the visual servoing is the orientation control. In the hot-swap system, it is necessary for the UAV to land with a specific orientation, which can be predefined as θ

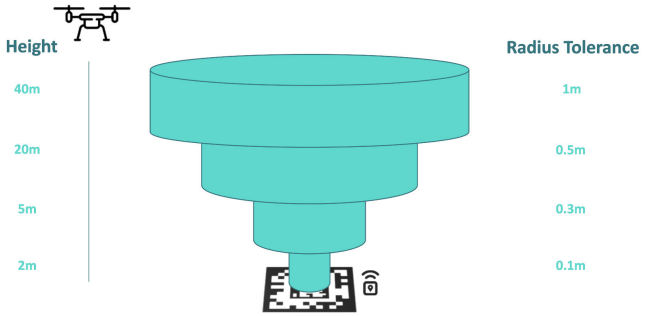

FIGURE 9. Z-axis controller conditions. Descent is permitted once the green zone is reached.

based on the marker's position. This allows for the orientation error calculated as

$$\mathbf{E}_w = m_\theta - \theta, \tag{7}$$

where m_θ is the yaw angle obtained from the marker's pose estimation. Analog to the equation (8), the yaw control action is derived using

$$\mathbf{V}_w = \alpha\sigma(E_w). \tag{8}$$

D. OPTICAL ENHANCEMENT

The visual servoing method described in subsection IV-C relies on the execution of pose estimation. Given the necessity for long-distance operations in the proposed system, optical enhancement techniques are employed to ensure real-time detection when the marker is within the frame.

In terms of hardware, the camera DJI Zenmuse H20T is chosen, which offers 23x hybrid optical zoom capability. Leveraging this feature, a zoom-level controller is implemented. To initiate this control, the first step involves determining the camera's field of view (FOV) using sensor parameters such as focal length (f) and sensor size (s). This calculation can be expressed as follows:

$$\text{FOV} = 2tan^{-1}\left(\frac{s}{2f}\right). \tag{9}$$

With the FOV known, it becomes possible to estimate the visible swath ($2d$) within the camera frame using trigonometry, as shown in Figure 10. The equation for this estimation is:

$$d = h \cdot tan\left(\frac{\text{FOV}}{2}\right), \tag{10}$$

where h represents the UAV relative height to the marker, which can be obtained either through pose estimation or from the drone's GPS height when pose data is unavailable. By defining a desired range of d, the controller employs the relative height as the main parameter for determining the appropriate zoom level.

The transition between different zoom levels in the controller is a dynamic process that takes a matter of hundreds of milliseconds. This rapid switching may have implications for pose estimation, especially when it is performed continually during the landing phase.

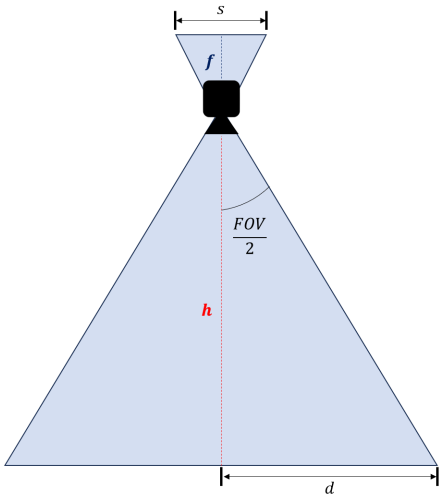

FIGURE 10. Estimation of visible swath ($2d$) based on sensor parameters and relative distance (h).

To address this challenge, the concept of cylindrical zones arranged in a cone shape, as shown in Figure 9, plays a pivotal role in the zoom-level controller's operation. Each border of these cylindrical zones corresponds to a change in various controller parameters, including zoom level, radius tolerance (as defined in Equation 4), and z-velocity (as specified in Equation 6).

In Table 1, we present the details of the implemented zones and the corresponding controller parameters. These sensor transitions were designed with the objective of achieving a minimum ground radius coverage of 5 meters, which helps compensate for potential GPS inaccuracies. Therefore, Table 1 provides information on the visible ground width and height at each transition zone.

With all the processing being executed on the edge computer, the high-definition images (1920 × 1440) at 30 frames-per-second may add some delay to the system as the UAV approaches the marker. In order to reduce this impact a prediction model is employed.

Each fractal inference yields two sets of outputs: a 6-degree-of-freedom (6-DOF) pose in the camera frame and a 2-DOF polygon array in the image frame. Considering the marker illustrated in Figure 7, it is reasonable to assume the presence of three possible polygons within the array. In order to optimize the system's performance, the smallest polygon is selected for the prediction model.

Assuming that during the landing phase the landing pad's relative movement between frames is very small, the center and area of the last estimation can be used to reduce significantly the size of the image. Adding a margin of 10% at the area of the polygon, the prediction model is able to cover most of the relative movement that happens during the 30 ms period between frames.

V. TRIALS AND DISCUSSIONS

The RAPID project conducted its test campaigns at two key locations: an airfield on the coast of Wicklow, Ireland, and the Port of Hamburg, Germany. This section details the

TABLE 1. Descending cone-based region zones.

Height	Sensor	Width	Height	Tolerance	v_z
3 m	Wide	4 m	3 m	0.1 m	0.25 m/s
7 m	Wide	10 m	7 m	0.5 m	1.25 m/s
	2x Zoom	7 m	6 m		
21 m	2x Zoom	22 m	17 m	1 m	2.5 m/s
	3x Zoom	14 m	10 m		
28 m	3x Zoom	18 m	14 m	2 m	2.5 m/s
	5x Zoom	11 m	8 m		
35 m	5x Zoom	13 m	10 m	2 m	2.5 m/s
	7x Zoom	9 m	7 m		
49 m	7x Zoom	13 m	10 m	2.5 m	2.5 m/s
	10x Zoom	9 m	7 m		
63 m	10x Zoom	12 m	9 m	2.5 m	2.5 m/s
	12x Zoom	10 m	7 m		
77 m	12x Zoom	12 m	9 m	3 m	2.5 m/s
	17x Zoom	8 m	6 m		
93 m	17x Zoom	10 m	8 m	3 m	2.5 m/s
	20x Zoom	8 m	6 m		

trials of the developed cooperative system, with the proposed landing approach being validated during the Wicklow trials. Additionally, a comprehensive deployment of the cooperative solution was executed to inspect a lock at the Port of Hamburg.

A. WICKLOW - LANDING PHASE

In April 2022, a series of trials were carried out in Wicklow, Ireland, as part of the RAPID project's development and validation process. The primary focus of these trials was to rigorously assess the performance of the landing phase within the cooperative UAV-USV system. To achieve this, a controlled testing environment was established, enabling the emulation of the USV's GPS position over the network.

During these trials, the team sought to emulate real-world scenarios where the UAV was engaged in operations at different locations. The objective was to investigate the seamless transition from the operational phase to the landing phase, specifically when the UAV had completed tasks at different sites and needed to initiate the landing procedure.

The trials were designed to assess the system's ability to execute precise and efficient landings based on the emulated USV GPS position. These trials not only validated the technical aspects of the landing phase but also served as a critical step in ensuring the overall effectiveness and safety of the cooperative UAV-USV system for extended coverage of maritime operations.

As shown in Figure 11, the drone initiates the landing phase from a randomly selected point within the operational area, heading towards the designated takeoff/landing location. The target GPS coordinate is broadcasted through a WiFi access point (AP), which the UAV can access either via a cloud-based server or the RF link. This deliberate ambiguity is intentionally designed to introduce an additional layer of safety into the system, particularly in the event of a connection loss.

Following the landing request, the workflow described in Figure 6 is initiated. A comprehensive graph illustrating

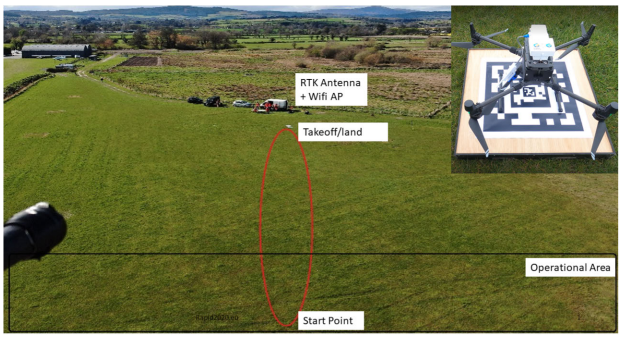

FIGURE 11. Wicklow trial environment.

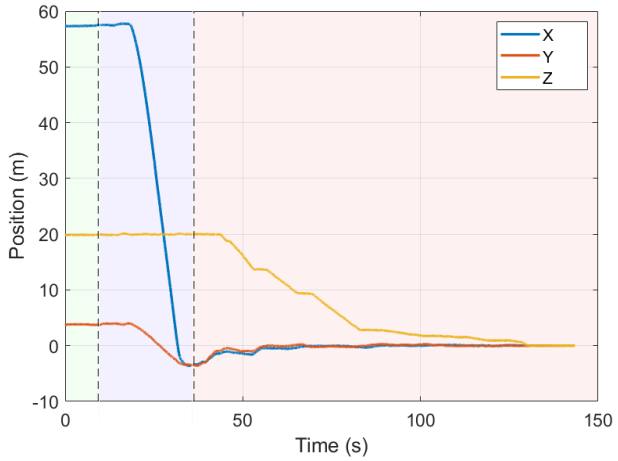

FIGURE 12. Relative position (x, y, z) between the UAV and landing pad during landing phase: Green (Before landing request), Blue (GPS-Based controller), Red (Visual Servoing).

the relative position (x, y, z) between the UAV and the landing pad over time is presented in Figure 12. This graph provides a visual representation of the system's performance, showcasing how errors on each axis change as time progresses. The relative error was assessed by calculating the difference between the GPS position of the landing pad and the GPS position, with RTK corrections, throughout the entire flight.

Figure 12 highlights three distinct stages: The green area denotes the initial operation phase, which transitions to the landing request phase. Once the request is initiated, the blue area represents the approach phase, controlled by GPS. Before acting towards a GPS position, the controller initiates corrections for both the yaw position to face the target coordinate and the height to a specific level, which is predetermined based on the operational surroundings to increase safety. When a visual-based detection is achieved, the system starts the descent phase, depicted in the red area. A clip for this trial is available at **Wicklow Trial**.

The emulated operation is conducted approximately 60 meters from the USV. Before progressing to the visual servoing phase, the approach phase accumulates an error of 4.8684 m, which can be attributed to GPS inaccuracies. During the descending phase, it is possible to observe the proposed zone transitions (Figure 9) and time-window (Equation 5) in the z-axis. This is a crucial feature due to

TABLE 2. Landing results.

Trial	n	Height	Accuracy	Time	Environment
University of Limerick - April 2022	#1	14 m	12.21 cm	75 s	Clear and Calm Wind
	#2	15 m	14.56 cm	120 s	
	#3	15 m	8.24 cm	54 s	
Wicklow - April 2022	#1	28 m	8.24 cm	75 s	Light rain and Wind gusts
	#2	22 m	12.20 cm	65 s	
	#3	14 m	33.01 cm	58 s	
	#4	14 m	6.40 cm	95 s	
	#5	14 m	6.70 cm	105 s	
	#6	21 m	9.43 cm	53 s	
	#7	31 m	4.12 cm	132 s	
	#8	26 m	6.71 cm	73 s	
	#9	26 m	7.07 cm	67 s	
	#10	20 m	6.71 cm	92 s	
Port of Hamburg - September 2022	#1	9 m	3.60 cm	69 s	Clear and Calm Wind + Water Surrounding
	#2	7 m	9.22 cm	68 s	
	#3	11 m	7.62 cm	47 s	
	#4	9 m	6.40 cm	57 s	
	#5	10 m	8.06 cm	55 s	
University of Limerick - December 2022	#1	20 m	7.07 cm	32 s	Low-light and calm wind
	#2	20 m	8.25 cm	60 s	
	#3	26 m	11.66 cm	73 s	
	#4	16 m	9.05 cm	45 s	
	#5	20 m	0.08 cm	41 s	
Port of Hamburg - June 2023	#1	7 m	0.60 cm	33 s	Rain and Calm Wind + Water Surrounding
	#2	13 m	12.08 cm	23 s	
	#3	19 m	13.04 cm	27 s	
University of Limerick - October 2023	#1	60 m	7.99 cm	38 s	Low-light and Wind gusts
	#2	60 m	8.25 cm	43 s	
	#3	60 m	9.95 cm	41 s	
	#4	80 m	18.05 cm	47 s	
	#5	80 m	7.43 cm	52 s	
	#6	100 m	14.51 cm	67 s	

the fact that at higher altitudes small variations at the marker center estimation can result in a huge pose error.

Lastly, it is crucial to emphasize the choice of employing a different descending velocity for the final 5 m of the descent. This decision is driven by the specific challenges presented in the maritime context, where the limited landing space on the USV poses a high risk of an unintended water landing. In the event of a sudden wind gust, a rapid descent could lead to a failed landing, potentially resulting in the loss of the UAV.

The deployment of the landing approach proved to be a resounding success, having been executed over 50 separate occasions across a spectrum of challenging conditions and different scenarios. These comprehensive trials encompassed varying weather conditions, including both clear skies and rainy weather. Moreover, the system demonstrated its resilience even in the face of fluctuating wind speeds, with some instances featuring gusts of up to 12 meters per second (m/s).

This extensive testing and remarkable consistency underscore the robustness and adaptability of the cooperative UAV-USV system. It is worth noting that a total of 29 meticulously documented landing attempts have been recorded throughout the trials, with corresponding data available in ROSBAG files accessible through the **Landing-UAV** dataset. These resources offer valuable insights into the system's performance, serving as an essential repository for further analysis and research.

Table 2 provides a comprehensive summary of the results obtained from the documented landing attempts within the cooperative UAV-USV system. The table offers detailed information on key performance metrics, including Height (m), landing accuracy (cm), and Time (s), which are critical in assessing the system's reliability and efficiency. It is noteworthy that accuracy is defined based on post-processed measurements extracted from the last frame of the gimbaled camera facing down, estimating the distance from the center of the camera to the center of the marker. Moreover, Table 2

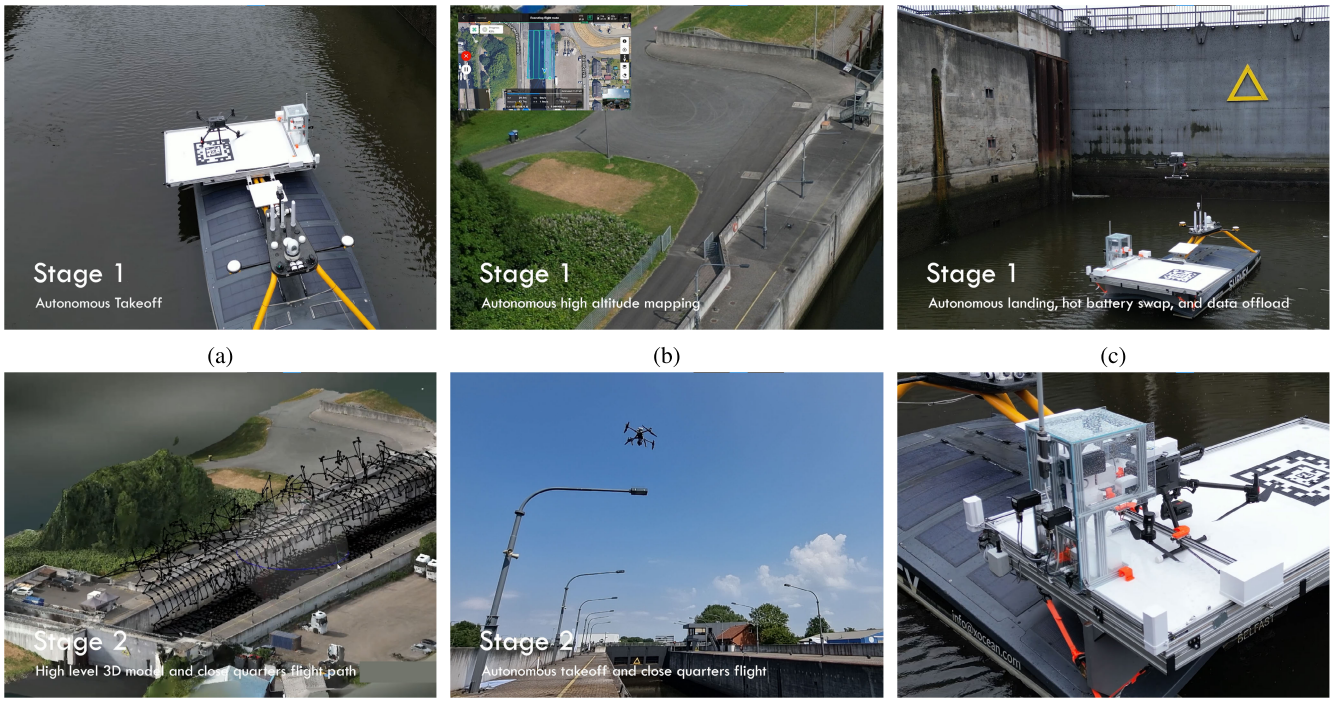

FIGURE 13. A visual journey of the cooperative system in action. (a) Autonomous takeoff, (b) High-Altitude mapping, (c) autonomous landing, Hot-Swap, and data offload, (d) High-Level 3D model and close quarters flight path, (e) Close quarter flights, (f) UAV securely locked onto the USV.

provides information about environmental factors, such as weather conditions and terrain characteristics surrounding the landing pad, which can significantly impact the landing process.

In fact, changes in the landing time observed in Table 2 are derived from factors such as low-light conditions that could lead to a reduction in the number of detections. Additionally, variations in wind and the presence of a movable target (USV on the water) affect the time the UAV spends in the cone-shaped region (Figure 9). These environmental factors impact the descending approach, particularly as it relies on a certain number of detections within a specified time window, as defined in equation (5).

Another critical factor influencing system performance is the error in pose estimation, which is directly proportional to the height of the UAV. Increased error levels can result in less smooth controller actions, posing potential challenges at higher altitudes. Nevertheless, it's important to note that, within the current regulatory limits, the system's configuration has experienced only minor effects.

In the early stages of the system's development (From April 2022 until September 2022), we encountered a challenge related to frame dropout. This issue was primarily attributed to delays introduced by the pose estimation process, which, in turn, affected the decoding phase and occasionally led to a pixelation effect in the captured frames. During this initial period, the average landing time was 75.5 s, and the average landing height was approximately 17 m.

To address this frame dropout issue and enhance the system's performance, we implemented the prediction model detailed in Section IV-D for the remaining trials. This model proved to be an effective solution for mitigating frame dropout, thereby improving the overall efficiency and accuracy of the landing procedure. In Fact, Table 3 presents a comprehensive overview, including the average, minimum, and maximum values recorded across the landing attempts of the final system design.

TABLE 3. Results summary of final system design - Since December 2022.

Landing Phase	Average	Minimum	Maximum
Height (m)	41.5	7	100
Accuracy (cm)	9.14	0.08	18.05
Time (s)	44.43	23	73

An improvement of 41% at landing time even with an average height more than 2 times bigger can be highlighted. The height range covered by the system extends from 7 m to 100 m, showcasing the remarkable capabilities of autonomous zoom-level control. As a result, the cooperative system can be fully operational within a mere 5 minutes after the UAV reaches the USV's GPS position, with an additional 2 minutes allocated for the landing phase and up to 3 minutes for the hot-swap.

B. PORT OF HAMBURG - COOPERATIVE SYSTEM

In June 2023, a pivotal phase of the RAPID project unfolded as a series of trials took place in the Port of Hamburg, Germany. The primary objective of these trials was to showcase the cooperative UAV-USV system as a fully integrated and comprehensive solution for maritime operations. The trials

represented a significant milestone as they incorporated the entire operational workflow, culminating in the inspection of a lock within the Port of Hamburg, as described in Figure 13.

The initial step in the operation involves positioning the USV at the inspection location. Upon reaching the lock, the UAV is then relocated to its designated takeoff position, initiating the mission, as shown in Figure 13a. In alignment with the approach outlined in [19] for inspecting unknown structures, the trial commenced with a high-altitude mapping flight, as depicted in Figure 13b. This flight provided a comprehensive overview of the target area, encompassing the specific lock within the Port of Hamburg. Subsequently, the landing phase was executed, followed by a battery hot-swap to ensure uninterrupted operations, as illustrated in 13c.

Following the successful landing phase, the collected data is promptly offloaded to a ground station via a cloud-based server. This data is then utilized to generate a low-resolution mesh of the area encompassing the target of interest. This mesh serves as the foundation for secure close-quarters path planning, ensuring precise and controlled navigation, as shown in Figure 13d.

With the second mission ready, the UAV is deployed to perform a close-quarter survey of the lock, offering a comprehensive and intricate examination of this vital maritime structure, as shown in Figure 13e. Once the survey is completed, the UAV proceeds to initiate the landing phase. The culmination of the mission is achieved when the UAV securely locks onto the USV, as illustrated in Figure 13f. A clip for this trial is available at **RAPID Final Demo**.

It is worth mentioning that during the trials, pilots were present to supervise the operations, in accordance with current legislation. Nevertheless, every step executed by the cooperative system was fully automated. These trials validated the cooperative system's ability to operate seamlessly and effectively in maritime port scenarios.

The incorporation of the hot-swap system, combined with the impressive endurance of the USV lasting up to 2 days, positions the UAV for swift deployment in subsequent missions. As an inspection use case, once a high-resolution model is constructed in the second stage, the system could leverage AI models to detect structural cracks. Specific locations of interest can then be revisited for a sub-millimeter survey, further enhancing the system's capabilities in maintaining and monitoring critical maritime infrastructure.

VI. CONCLUSION

The cooperative UAV-USV system developed as part of the RAPID project has demonstrated its potential as a versatile and effective solution for extending the coverage of maritime operations. The successful trials conducted in both Wicklow, Ireland, and the Port of Hamburg, Germany, have showcased the system's robustness and adaptability across a range of challenging scenarios, including varying weather conditions and fluctuating wind speeds.

The ability of the system to seamlessly transition from high-altitude mapping flights to close-quarter surveys is a testament to its flexibility and precision. The hot-swap of batteries further enhances its operational endurance, ensuring the system's readiness for extended missions while allowing for uninterrupted continuous surveys.

Moreover, the deliberate introduction of safety measures, such as ambiguity in the landing approach, adds an additional layer of reliability, making the cooperative system suitable for use in critical maritime environments.

The comprehensive data collected from the 29 documented landings provides valuable insights into the system's performance. These insights can inform future refinements and optimizations to further enhance the system's effectiveness.

In conclusion, the autonomous cooperative UAV-USV system represents a significant advancement in the field of maritime operations, enabling safer and more efficient inspections of critical infrastructure. With its successful deployment and demonstrated capabilities, it stands as a promising solution for a wide range of applications in the maritime industry. Future works may investigate the installation of a stabilization platform and safe landing approach for a sea state higher than three.

REFERENCES

[1] I. Lebedev, A. Erashov, and A. Shabanova, "Accurate autonomous UAV landing using vision-based detection of Aruco-marker," in *Proc. Int. Conf. Interact. Collaborative Robot.* Cham, Switzerland: Springer, 2020, pp. 179–188.

[2] A. Gautam, P. B. Sujit, and S. Saripalli, "A survey of autonomous landing techniques for UAVs," in *Proc. Int. Conf. Unmanned Aircr. Syst. (ICUAS)*, May 2014, pp. 1210–1218.

[3] A. Krystosik-Gromadziñska, "The use of drones in the maritime sector–areas and benefits," *Zeszyty Naukowe Akademii Morskiej W Szczecinie*, vol. 161, no. 67, pp. 45–55, 2021. [Online]. Available: https://bibliotekanauki.pl/articles/2033624.pdf

[4] S. Jordan, J. Moore, S. Hovet, J. Box, J. Perry, K. Kirsche, D. Lewis, and Z. T. H. Tse, "State-of-the-art technologies for UAV inspections," *IET Radar, Sonar Navigat.*, vol. 12, no. 2, pp. 151–164, Feb. 2018.

[5] V. E. Schneider, C. Nok Au, A. Budak, J. Oeffner, and J. Riordan, "Automated battery hot swap system that integrates unmanned aerial vehicles with the autonomous surface vehicle SeaML: SeaLion in port environment," in *Proc. OCEANS Limerick*, Jun. 2023, pp. 1–8.

[6] J. Wu, R. Li, J. Li, M. Zou, and Z. Huang, "Cooperative unmanned surface vehicles and unmanned aerial vehicles platform as a tool for coastal monitoring activities," *Ocean Coastal Manage.*, vol. 232, Feb. 2023, Art. no. 106421.

[7] G. Dooly, E. Omerdic, J. Coleman, L. Miller, A. Kaknjo, J. Hayes, J. Braga, F. Ferreira, H. Conlon, H. Barry, J. Marcos-Olaya, T. Tuohy, J. Sousa, and D. Toal, "Unmanned vehicles for maritime spill response case study: Exercise cathach," *Mar. Pollut. Bull.*, vol. 110, no. 1, pp. 528–538, Sep. 2016.

[8] Y. Ma, Y. Zhao, X. Qi, Y. Zheng, and R. Gan, "Cooperative communication framework design for the unmanned aerial vehicles-unmanned surface vehicles formation," *Adv. Mech. Eng.*, vol. 10, no. 5, May 2018, Art. no. 168781401877366.

[9] O. Araar, N. Aouf, and I. Vitanov, "Vision based autonomous landing of multirotor UAV on moving platform," *J. Intell. Robotic Syst.*, vol. 85, no. 2, pp. 369–384, Feb. 2017.

[10] M. A. Olivares-Méndez, I. F. Mondragón, P. Campoy, and C. Martínez, "Fuzzy controller for UAV-landing task using 3D-position visual estimation," in *Proc. Int. Conf. Fuzzy Syst.*, Jul. 2010, pp. 1–8.

[11] K. Máthé and L. Buşoniu, "Vision and control for UAVs: A survey of general methods and of inexpensive platforms for infrastructure inspection," *Sensors*, vol. 15, no. 7, pp. 14887–14916, Jun. 2015.

[12] F. J. Romero-Ramirez, R. Muñoz-Salinas, and R. Medina-Carnicer, "Speeded up detection of squared fiducial markers," *Image Vis. Comput.*, vol. 76, pp. 38–47, Aug. 2018.
[13] Z. Wang, B. Wang, C. Tang, and G. Xu, "Pose and velocity estimation algorithm for UAV in visual landing," in *Proc. 39th Chin. Control Conf. (CCC)*, Jul. 2020, pp. 3713–3718.
[14] C. Zhang, Y. Zou, F. Wang, E. del Rey Castillo, J. Dimyadi, and L. Chen, "Towards fully automated unmanned aerial vehicle-enabled bridge inspection: Where are we at?" *Construct. Building Mater.*, vol. 347, Sep. 2022, Art. no. 128543.
[15] K. Telli, O. Kraa, Y. Himeur, A. Ouamane, M. Boumehraz, S. Atalla, and W. Mansoor, "A comprehensive review of recent research trends on unmanned aerial vehicles (UAVs)," *Systems*, vol. 11, no. 8, p. 400, Aug. 2023.
[16] (2023). *Dji Dock Automated Drone Hangar Dji Enterprise*. [Online]. Available: https://enterprise.dji.com/dock
[17] (2023). *Drone Inspections for Industries - Automated & Bvlos Approved*. [Online]. Available: https://www.energy-robotics.com/inspection-drones
[18] (2023). *Technology Perceptual Robotics*. [Online]. Available: https://www.perceptual-robotics.com/technology/
[19] B. Bartlett, P. Trslic, M. Santos, M. Manduhu, J. Riordan, and G. Dooly, "Automated close-quarter, high-resolution inspection and 3D reconstruction of unknown infrastructure," in *Proc. OCEANS Limerick*, Jun. 2023, pp. 1–6.
[20] N. Vigne, R. Barrère, B. Blanck, F. Steffens, C. N. Au, J. Riordan, and G. Dooly, "Embedded port infrastructure inspection using artificial intelligence," in *Proc. OCEANS Limerick*, Jun. 2023, pp. 1–8.
[21] J. Ramos, R. Ribeiro, D. Safadinho, J. Barroso, C. Rabadão, and A. Pereira, "Distributed architecture for unmanned vehicle services," *Sensors*, vol. 21, no. 4, p. 1477, Feb. 2021.
[22] P. C. Santos, R. C. S. Freire, E. A. N. Carvalho, L. Molina, E. O. Freire, M. C. Santos, A. Weir, P. Trslic, E. Omerdic, G. Dooly, and D. Toal, "Fully automatic visual servoing control for underwater vehicle manipulator systems based on a heuristic inverse kinematics," *J. Intell. Robotic Syst.*, vol. 107, no. 3, p. 42, Mar. 2023.
[23] T. Yang, Z. Jiang, R. Sun, N. Cheng, and H. Feng, "Maritime search and rescue based on group mobile computing for unmanned aerial vehicles and unmanned surface vehicles," *IEEE Trans. Ind. Informat.*, vol. 16, no. 12, pp. 7700–7708, Dec. 2020.
[24] E.-J. Kim, S.-H. Nam, J.-W. Koo, and T.-M. Hwang, "Hybrid approach of unmanned aerial vehicle and unmanned surface vehicle for assessment of chlorophyll—A imagery using spectral indices in stream, South Korea," *Water*, vol. 13, no. 14, p. 1930, Jul. 2021.
[25] S. Jung, H. Cho, D. Kim, K. Kim, J.-I. Han, and H. Myung, "Development of algal Bloom removal system using unmanned aerial vehicle and surface vehicle," *IEEE Access*, vol. 5, pp. 22166–22176, 2017.
[26] P. Ozog, M. Johnson-Roberson, and R. M. Eustice, "Mapping underwater ship hulls using a model-assisted bundle adjustment framework," *Robot. Auto. Syst.*, vol. 87, pp. 329–347, Jan. 2017.
[27] C. A. Mueller, T. Fromm, H. Buelow, A. Birk, M. Garsch, and N. Gebbeken, "Robotic bridge inspection within strategic flood evacuation planning," in *Proc. OCEANS Aberdeen*, Jun. 2017, pp. 1–6.
[28] J. Gancet, D. Urbina, P. Letier, M. Ilzokvitz, P. Weiss, F. Gauch, G. Antonelli, G. Indiveri, G. Casalino, A. Birk, M. F. Pfingsthorn, S. Calinon, A. Tanwani, A. Turetta, C. Walen, and L. Guilpain, "DexROV: Dexterous undersea inspection and maintenance in presence of communication latencies," *IFAC-PapersOnLine*, vol. 48, no. 2, pp. 218–223, 2015.
[29] G. A. Hollinger, B. Englot, F. S. Hover, U. Mitra, and G. S. Sukhatme, "Active planning for underwater inspection and the benefit of adaptivity," *Int. J. Robot. Res.*, vol. 32, no. 1, pp. 3–18, Jan. 2013.
[30] Y. Han and W. Ma, "Automatic monitoring of water pollution based on the combination of UAV and USV," in *Proc. IEEE 4th Int. Conf. Electron. Inf. Commun. Technol. (ICEICT)*, Aug. 2021, pp. 420–424.
[31] G. Shao, Y. Ma, R. Malekian, X. Yan, and Z. Li, "A novel cooperative platform design for coupled USV–UAV systems," *IEEE Trans. Ind. Informat.*, vol. 15, no. 9, pp. 4913–4922, Sep. 2019.
[32] M. Chen, X. Zhang, X. Xiong, F. Zeng, and W. Zhuang, "Transformer: A multifunctional fast unmanned aerial Vehicles–Unmanned surface vehicles coupling system," *Machines*, vol. 9, no. 8, p. 146, Jul. 2021.
[33] Y. Yuan, X. Xu, H. Duan, Z. Zeng, D. Xu, R. Chen, and T. Wu, "Eagle vision-based coordinate landing control framework of unmanned aerial vehicles on an unmanned surface vehicle," *Guid., Navigat. Control*, vol. 2, no. 4, Dec. 2022, Art. no. 2250023.
[34] H. Niu, Z. Ji, P. Liguori, H. Yin, and J. Carrasco, "Design, integration and sea trials of 3D printed unmanned aerial vehicle and unmanned surface vehicle for cooperative missions," in *Proc. IEEE/SICE Int. Symp. Syst. Integr. (SII)*, Jan. 2021, pp. 590–591.
[35] H.-T. Zhang, B.-B. Hu, Z. Xu, Z. Cai, B. Liu, X. Wang, T. Geng, S. Zhong, and J. Zhao, "Visual navigation and landing control of an unmanned aerial vehicle on a moving autonomous surface vehicle via adaptive learning," *IEEE Trans. Neural Netw. Learn. Syst.*, vol. 32, no. 12, pp. 5345–5355, Dec. 2021.
[36] R. Acuna, D. Zhang, and V. Willert, "Vision-based UAV landing on a moving platform in GPS denied environments using motion prediction," in *Proc. Latin Amer. Robotic Symp., Brazilian Symp. Robot. (SBR) Workshop Robot. Educ. (WRE)*, Nov. 2018, pp. 515–521.
[37] J. Wubben, F. Fabra, C. T. Calafate, T. Krzeszowski, J. M. Marquez-Barja, J.-C. Cano, and P. Manzoni, "A vision-based system for autonomous vertical landing of unmanned aerial vehicles," in *Proc. IEEE/ACM 23rd Int. Symp. Distrib. Simul. Real Time Appl. (DS-RT)*, Oct. 2019, pp. 1–7.
[38] Q. Lu, B. Ren, and S. Parameswaran, "Shipboard landing control enabled by an uncertainty and disturbance estimator," *J. Guid., Control, Dyn.*, vol. 41, no. 7, pp. 1502–1520, Jul. 2018.
[39] R. Acuna and V. Willert, "Dynamic markers: UAV landing proof of concept," in *Proc. Latin Amer. Robotic Symp., Brazilian Symp. Robot. (SBR) Workshop Robot. Educ. (WRE)*, Nov. 2018, pp. 496–502.
[40] T. Krajník, M. Nitsche, J. Faigl, P. Vaněk, M. Saska, L. Přeučil, T. Duckett, and M. Mejail, "A practical multirobot localization system," *J. Intell. Robotic Syst.*, vol. 76, nos. 3–4, pp. 539–562, Dec. 2014.
[41] A. Keipour, G. A. S. Pereira, R. Bonatti, R. Garg, P. Rastogi, G. Dubey, and S. Scherer, "Visual servoing approach to autonomous UAV landing on a moving vehicle," *Sensors*, vol. 22, no. 17, p. 6549, Aug. 2022.
[42] S. Del Pizzo, U. Papa, S. Gaglione, S. Troisi, and G. Del Core, "A vision-based navigation system for landing procedure," *ACTA IMEKO*, vol. 7, no. 2, p. 102, Jul. 2018.
[43] P. H. Nguyen, K. W. Kim, Y. W. Lee, and K. R. Park, "Remote marker-based tracking for UAV landing using visible-light camera sensor," *Sensors*, vol. 17, no. 9, p. 1987, Aug. 2017.
[44] K. E. Wenzel, A. Masselli, and A. Zell, "Automatic take off, tracking and landing of a miniature UAV on a moving carrier vehicle," *J. Intell. Robotic Syst.*, vol. 61, nos. 1–4, pp. 221–238, Jan. 2011.
[45] J. Riordan, M. Manduhu, J. Black, A. Dow, G. Dooly, and S. Matalonga, "LiDAR simulation for performance evaluation of UAS detect and avoid," in *Proc. Int. Conf. Unmanned Aircr. Syst. (ICUAS)*, Jun. 2021, pp. 1355–1363.
[46] A. Dow, M. Manduhu, G. Dooly, P. Trslić, B. Blanck, C. Knox, and J. Riordan, "Intelligent detection and filtering of swarm noise from drone acquired LiDAR data using PointPillars," in *Proc. OCEANS Limerick*, Jun. 2023, pp. 1–6.
[47] (2023). *Xocean Ocean Data, Delivered*. [Online]. Available: https://xocean.com/
[48] V. E. Schneider, C. N. Au, A. Budak, and J. Oeffner, "The development of a battery hot swap prototype for use on the autonomous surface vehicle SeaML: SeaLion," in *Proc. 14th Symp. High-Perform. Mar. Vehicles (HIPER)*, V. Bertram, Ed. 2022, pp. 249–261. [Online]. Available: https://publica.fraunhofer.de/handle/publica/430872
[49] F. J. Romero-Ramire, R. Muñoz-Salinas, and R. Medina-Carnicer, "Fractal markers: A new approach for long-range marker pose estimation under occlusion," *IEEE Access*, vol. 7, pp. 169908–169919, 2019.

MATHEUS C. SANTOS (Member, IEEE) received the bachelor's degree in computer engineering and the master's degree in electrical engineering from the Federal University of Sergipe (UFS), in 2019 and 2021, respectively. He is currently pursuing the Ph.D. degree in electrical engineering with the University of Limerick. He is also a member of the Centre of Robotics and Intelligent Systems (CRIS) and the Robotics Research Group (GPR), UFS.

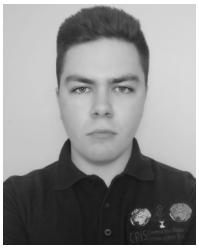

BEN BARTLETT (Member, IEEE) received the bachelor's degree (Hons.) in electronic and computer engineering from the University of Limerick, in 2021, where he is currently pursuing the Ph.D. degree with the Centre for Robotics and Intelligent Systems (CRIS). His research interests include the development of machine vision algorithms for detection and identification in aerial applications.

VINCENT E. SCHNEIDER received the bachelor's and master's degrees in science from Hochschule Bremen, in 2015 and 2017, respectively. Currently, he is a Research Associate with Sea Traffic and Nautical Solutions, Fraunhofer Center for Maritime Logistics and Services (CML).

FIACHRA Ó. BRÁDAIGH received the bachelor's degree in aeronautical engineering from the University of Limerick, in 2001, and the Master of Science degree in computer aided mechanical and manufacturing engineering from Dublin City University. Currently, he is a Research and Development Mechanical Engineer with XOCEAN, where they continue to push the boundaries of innovation in ocean data delivery.

BENJAMIN BLANCK received the bachelor's degree in business informatics. He is currently pursuing the master's degree in IT management and consulting with the University of Hamburg. He is also an accomplished Project Manager of the Hamburg Port Authority, specializing in research and development. With a Certified Scrum Master (PSM1), they are dedicated to leading innovative projects.

PHILLIPE C. SANTOS received the bachelor's degree in electronic engineering and the master's degree in electrical engineering from the Federal University of Sergipe (UFS), in 2015 and 2017, respectively, and the Ph.D. degree in electrical engineering from the Federal University of Campina Grande, in 2021. Currently, he is a Professor with the Federal Institute of Sergipe and a member of the Robotics Research Group (GPR), UFS, and the Centre for Robotics and Intelligent Systems, University of Limerick.

PETAR TRSLIC received the B.Sc. and M.Sc. degrees in mechanical engineering from the University of Zagreb and the Ph.D. degree from the University of Limerick (UL), in March 2020. He is currently a Postdoctoral Researcher with CRIS, UL. During the Ph.D. degree, he was working on the development of advanced monitoring, control systems and onboard robotics for the automation of MRE inspection, repair, and maintenance.

JAMES RIORDAN received the Ph.D. degree in underwater sonar modelling and simulation from the University of Limerick, Ireland. He specializes in robotics and sensing and an Expert in autonomous vehicles applied to land, air, and sea domains. He is currently a Reader with the University of the West of Scotland, where he leads an €8 million portfolio of research projects as a Principal Investigator and the founding Director of the ALMADA Research Centre. He is also a PI of the European Commission H2020 Project RAPID and an Independent External Expert to the European Union Aviation Safety Agency. He has established and successfully commercialized several strands of patented research and has been recipient of three national awards for research and innovation.

GERARD DOOLY (Member, IEEE) received the bachelor's degree in electronic and computer engineering and the Ph.D. degree from the University of Limerick (UL), Ireland, in 2003 and 2008, respectively, working with optical-based sensor systems. He is currently a Lecturer in digital technologies with UL, where he has worked extensively in robotics for over 20 years. He is also the Co-Director of the CRIS Centre and is an Investigator with the SFI Centre for Smart Manufacturing, CONFIRM, and the SFI MaREI Centre for Energy, Climate, and the Marine. He is the nominated responsible person for UAS operations within CRIS and holds a license to pilot up to 75KG MTOW fixed wing or multirotor UAS from the Irish Aviation Authority. His research interests include real-time 3D reconstruction, machine vision and machine learning, optical sensors, structural health monitoring, and automated survey and intervention. He is focused on the design and development of robotics and has led numerous multi-partner and multi-agency projects both here in Ireland and on the continent.